ISSN:

Effect of the Magnetic Field and Rotation on Peristaltic Flow of A Bingham Fluid in Asymmetric Channel with Porous Medium

Mohammed Obayes Kadhim*, Liqaa Z. Hummady
Department of Mathematics, College of Science, University of Baghdad, Baghdad, Iraq

Received: 27/12/2022 Accepted: 14/4/2023 Published: 30/3/2024

Abstract

In this paper, we investigate the influence of the rotation and magnetic field on the peristaltic flow of the Bingham fluid in an asymmetric channel with a porous medium under the long wavelength and low Reynolds number approximation assumptions. The perturbation method and the Mathematica program for solving nonlinear partial differential equations are used to couple the momentum equations with the rotational and magnetic field equations. The fluid is considered to be subject to a magnetic field and to flow within a porous medium. Graphs are used to display expressions for speed, stress gradient, magnetic subject, current density, rotation impact, and drift function. The findings reveal that the rotation, density, permeability, coupling diversity, and non-dimensional wave amplitude all play significant roles in the phenomenon. The quantities flow has been tested for variant parameters. The impact of the Bingham, Hartman and Darcy numbers are also tested for different values to indicate the effect on the movement of flow fluid. The applications can be seen through many graphics.

Keywords: Peristaltic flow, Rotation, Magnetic field, Bingham.

تأثير المجال المغناطيسي والدوران على التدفق التمعجي لسائل بينغهام في قناة غير متماثلة بوسط مسامي

محمد عبيس كاظم، لقاء زكي حمادي
قسم الرياضيات، كلية العلوم، جامعة بغداد، بغداد، العراق

الخلاصه

في هذا البحث، قمنا بدراسة تأثير الدوران والمجال المغناطيسي على التدفق التمعجي لسائل بينغهام في قناة غير متناظرة ذات وسط مسامي تحت الطول الموجي الطويل وافتراضات تقريب رقم رينولدز المنخفضة. يتم استخدام طريقة الاضطراب وبرنامج الرياضيات لحل المعادلات التفاضلية الجزئية غير الخطية لربط معادلات الزخم مع معادلات المجال الدوراني والمغناطيسي. يعتبر السائل خاضعًا لمجال مغناطيسي ويتدفق داخل وسط مسامي. تُستخدم الرسوم البيانية لعرض تعبيرات عن السرعة وتدرج الضغط والموضوع المغناطيسي وكثافة التيار وتأثير الدوران ووظيفة الانجراف. تكشف النتائج أن الدوران والكثافة والنفاذية وتنوع الاقتران وسعة الموجة غير الأبعاد تلعب جميعها أدوارًا مهمة في هذه الظاهرة. تم اختبار تدفق الكميات للمعلمات المتغيرة. يتم أيضًا اختبار تأثير أرقام Bingham وHartman وDarcy لقيم مختلفة للإشارة إلى التأثير على حركة مائع التدفق. يمكن رؤية التطبيقات من خلال العديد من الرسومات.

*Email: m.m.96moh@gmil.com

1. Introduction

A fluid waft mechanism that is known as peristaltic transport is approximately delivered with the aid of the propagation of wave trains alongside the channel partitions. This phenomenon has several real-world applications in body structure and biomedical engineering, which include food swallowing, blood drift inside the bile duct, lymph drive inside the lymphatic arteries, urine delivery thru the ureter, chyme motion inside the digestive machine, and ovum transport, etc. Initially Latham [1] and Shapiro et al. Burns and Parkes [2] used two situations to analyze peristaltic transport; the first example uses the peristaltic flow without pressure gradient, while the second involves flow down a channel or tube under pressure. In [3], the length wavelength, low Reynolds wide variety peristaltic pumping is utilized. Faraday and Richie are the first researchers who conduct a known experiment in which they tested the effects of magnetic fluid dynamics[4]. In [5], [6], [7], [8], [9], The peristaltic delivery of the fourth-grade fluid is investigated in connection to rotation, initial pressure, heat switch, and a prompted magnetic area, effects of rotation, initial stress and inclination of magnetic field on the axial velocity and pressure gradient that are discussed in detail. in addition, the closed form expressions for the stream function, pressure gradient, temperature, magnetic force function, induced magnetic field and current density are developed. Slippy flows which include the phase flows in porous slider bearings and flows thru pipes where chemical reactions take the area on the walls would be beneficial for the studies of problems in chemical engineering. The tapered asymmetric channel in the flow induced by talking peristaltic wave imposed on the non-uniform boundary walls to possess different amplitudes and phases [10]. The influence of heat and mass transfer on the peristaltic transport of viscoelastic fluid in presence of a magnetic field through a symmetric channel with the porous medium has been investigated [11]. The influence of the inclined magnetic field on the peristaltic transport of a non-Newtonian fluid in an anti-symmetric porous channel is discussed. The non-Newtonian fluid is a hyperbolic tangent fluid model [12]. Hatem studied the analysis of the effect of rotation on the analysis of heat transfer by mixed convection for the peristaltic transport of a viscous liquid in an asymmetric channel [13]. He also analyzed the effect of rotation and magnetic field on the analysis of heat transfer by mixed convection of a viscous liquid through a porous medium in an asymmetric. Another more difficult challenge is when using OCR to recognize mathematical expressions in the channel [14]. The obtained results are in agreement with Vajravelu et al. [15] and Sumalatha and Sreenadh [16] in a good way. For flows past stiff obstacles containing non-Newtonian fluids the no-slip boundary condition is often used. On strong borders, however, it has been discovered that a number of polymeric fluids stick-slip or slip. In those conditions, the fluid reveals a lack of adhesion on the wetted wall, inflicting it to slide along the wall and exhibit slip float behavior. The fluid displays non-continuum functions like slip waft when the molecular mean free-route period of the fluid is much like the gap between the plates (nanochannels or microchannels). By using the correct slip boundary conditions, the resulting equations are solved analytically. The effects of yield stress, amplitude ratio, Darcy number, slip parameter, and elastic parameters on flow are depicted in graphs. Medical professionals are now able to investigate blood flow in arteries much more effectively than before. The results of the current model also help with dialysis, heart-lung, and machine modeling, etc. Understanding the intricate physiological reaction of blood in the aforementioned settings is made easier by the results of the current model. Using a porous medium in an asymmetric channel, Investigating the effects of sliding and rotation on the peristaltic flow of Bingham fluid is the aim of this study. The examination of various parameter values occurs as the fluid travels through a two-dimensional tube. We look into electrical conduction to the fluid when a rotating magnetic field is presented. The velocity is also shown by using a variety of graphs and figures. We illustrate gradient pressure, stream function, magnetic force, stress at the lower and upper

channels, and induced magnetic and current density. Application of this work is used in the engineering field.

2. Mathematical Formulation for Asymmetric flow:

We think about the Bingham fluid flowing in two dimensions through an irregular conduit made of porous material. The cause of flow is caused by sinusoidal wave trains moving at a steady pace along the channel walls (c). The following factors describe the upper wall's surface:

$$\overline{h_1}(\bar{x},\bar{t}) = E_1 - r_1 \sin[\frac{2\pi}{\lambda}(\bar{x} - c\bar{t})] \quad \text{upper wall,} \tag{1}$$

while at the lower wall is given by.

$$\overline{h_2}(\bar{x},\bar{t}) = -E_2 - r_2 \sin[\frac{2\pi}{\lambda}(\bar{x} - c\bar{t}) + \emptyset] \quad \text{lower wall.} \tag{2}$$

where r_1 and r_2 indicate the wave's amplitudes, respectively. The E_1 and E_2 denote the channel's width, λ specifies the wavelength, The direction of the wave's propagation is represented by $\overline{X}$, while the time is indicated by $\bar{t}$. The difference in phase $\emptyset$ varies across the range $(0 \le \emptyset \le \pi)$ in which $\emptyset = 0$ is equivalent to an out-of-phase, asymmetric channel and $\emptyset = \pi$ stands for the phase of the waves. Further, r_1, r_2, E_1, E_2, and $\emptyset$ satisfy the following condition:

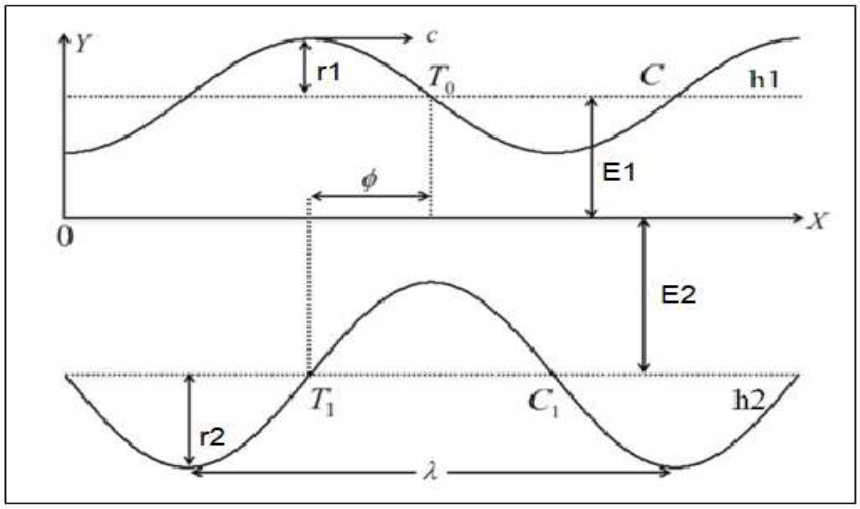

Figure 1: Cartesian Dimensional Asymmetric Coordinates.

$$r_1^2 + r_2^2 + 2r_1 r_2 \cos i(\emptyset) \le (E_1 + E_2)^2. \tag{3}$$

Furthermore, it is assumed that the walls don't move longitudinally. This assumption limits the ability of the walls to deform rather than implying that the channel is stiff during longitudinal motions.

3. Basic Equation

The fluid exhibits behavior consistent with the Bingham model, and the following information about its Cauchy stress tensor is given [17].

$$\sigma = -PI + \bar{S} . \tag{4}$$

where,

$$\bar{S} = 2\mu\tau + 2\tau_0\hat{\tau} . \tag{5}$$

In equation (5), τ_0 is the yield stress, and the tensor of the rate of deformation is τ . $\hat{\tau}$ is the tensor which is described as follows:

$$\hat{\tau} = \frac{\tau}{\sqrt{2\ tras\ \tau^2}} . \tag{6}$$

$$\tau = \frac{1}{2}(\nabla\overline{V} + (\nabla\overline{V})^{T}) \ . \quad (7)$$

Where I is the identifier tensor, $\overline{\nabla}=(\partial\overline{X}, \partial\overline{Y}, 0)$ the gradient vector, $\bar{P}$ is the liquid's pressure and μ is the dynamic viscosity.

$$\bar{s}_{\bar{x}\bar{x}} = 2\mu\bar{u}_{\bar{x}} + \frac{2\tau_0\bar{u}_{\bar{x}}}{\sqrt{2\bar{u}_{\bar{x}}^{\,2}+\left(\bar{v}_{\bar{x}}+\bar{u}_{\bar{y}}\right)^2+2\bar{v}_{\bar{y}}^{\,2}}} \ . \quad (8)$$

$$\bar{s}_{\bar{x}\bar{y}} = 2\mu\left(\frac{\bar{v}_{\bar{x}}+\bar{u}_{\bar{y}}}{2}\right) + \frac{2\tau_0\left(\frac{\bar{v}_{\bar{x}}+\bar{u}_{\bar{y}}}{2}\right)}{\sqrt{2\bar{u}_{\bar{x}}^{\,2}+\left(\bar{v}_{\bar{x}}+\bar{u}_{\bar{y}}\right)^2+2\bar{v}_{\bar{y}}^{\,2}}} \ . \quad (9)$$

$$\bar{s}_{\bar{y}y} = 2\mu\bar{v}_{\bar{y}} + \frac{2\tau_0\bar{v}_{\bar{y}}}{\sqrt{2\bar{u}_{\bar{x}}^{\,2}+\left(\bar{v}_{\bar{x}}+\bar{u}_{\bar{y}}\right)^2+2\bar{v}_{\bar{y}}^{\,2}}} \ . \quad (10)$$

4. The Governing Equation

The continuity equation may be used to illustrate the fundamental equations of motion in a peristaltic transport and magnetic of the Bingham fluid in experimental frame $(\bar{x}, \bar{y})$:

$$\frac{\partial\,\bar{u}}{\partial\bar{x}} + \frac{\partial\,\bar{v}}{\partial\bar{y}} = 0. \quad (11)$$

The $\bar{x}$ – part of the moment equation is:

$$\rho\left(\frac{\partial}{\partial\bar{t}} + \bar{u}\frac{\partial}{\partial\bar{x}} + \bar{v}\frac{\partial}{\partial\bar{y}}\right)\bar{u} - \rho\Omega\left(\Omega\bar{u} + 2\frac{\partial\,\bar{v}}{\partial\bar{t}}\right) = -\frac{\partial\bar{p}}{\partial\bar{x}} + \frac{\partial}{\partial\bar{x}}\bar{s}_{\bar{x}\bar{x}} + \frac{\partial}{\partial\bar{y}}\bar{s}_{\bar{x}\bar{y}} - \sigma B_0^2\bar{u} - \frac{\mu}{\bar{k}}\bar{u} \ . \quad (12)$$

The $\bar{y}$ – part of the moment equation is:

$$\rho\left(\frac{\partial}{\partial\bar{t}} + \bar{u}\frac{\partial}{\partial\bar{x}} + \bar{v}\frac{\partial}{\partial\bar{y}}\right)\bar{v} - \rho\Omega\left(\Omega\bar{v} + 2\frac{\partial\,\bar{u}}{\partial\bar{t}}\right) = -\frac{\partial\bar{p}}{\partial\bar{x}} + \frac{\partial}{\partial\bar{x}}\bar{s}_{\bar{x}\bar{y}} + \frac{\partial}{\partial\bar{y}}\bar{s}_{\bar{y}\bar{y}} - \sigma B_0^2\bar{v} - \frac{\mu}{\bar{k}}\bar{v} \ . \quad (13)$$

Where ρ , $\bar{p}, \mu, \bar{k}, B_0, \Omega$ are the constant density, pressure, dynamic viscosity, permeability parameter, constant magnetic field, and rotation, respectively. The $\bar{u}$ and $\bar{v}$ are the velocities in X and Y paths in a given frame.

The flow in the laboratory frame is erratic $(\bar{x}, \bar{y})$. Therefore, with a coordinate system traveling at the speed of wave c in wave frame $(\overline{X}, \overline{Y})$, the motion is steady. The following expressions

$$\bar{x} = \overline{X} - c\bar{t}\ , \bar{y} = \overline{Y}\ , \bar{u}(\overline{X}, \overline{Y}) = \overline{U}(\bar{x}, \bar{y}) - c\ , \bar{v}(\overline{X}, \overline{Y}) = \overline{V}(\bar{x}, \bar{y})\ , \overline{P}(\overline{X}) = \overline{P}(\bar{x}, \bar{t}). \quad (14)$$

where $\overline{u}, \overline{v}$ and $\overline{p}$ represent the velocity components and pressure in the wave frame, respectively. Set up the following non-dimensional quantities to perform the non-dimensional analysis:

$$x = \frac{1}{\lambda}\bar{x}\ , y = \frac{1}{d}\bar{y}\ , u = \frac{1}{c}\bar{u}\ , v = \frac{1}{\delta\,c}\bar{v}\ , t = \frac{c}{\lambda}\bar{t}\ , \delta = \frac{d}{\lambda}\ , Re = \frac{\rho\,c\,d}{\mu}, Da = \frac{\bar{k}}{d^2},$$

$$s_{xx} = \frac{\lambda}{\mu\,c}\bar{s}_{\bar{x}\bar{x}}\ , s_{xy} = \frac{d}{\mu\,c}\bar{s}_{\bar{x}\bar{y}}\ ,\ s_{yy} = \frac{d}{\mu\,c}\bar{s}_{\bar{y}\bar{y}}\ , M = \sqrt{\frac{\sigma B_0^2 d^2}{\mu}}, h_1 = \frac{1}{d}\overline{h_1}\ ,\ h_2 = \frac{1}{d}\overline{h_2}\ ,\ \beta = M^2 + \frac{1}{Da}\ , R_n = \frac{\tau_0 d}{\mu c}\ , p = \frac{d^2}{\lambda\mu\,c}\bar{p}\ . \quad (15)$$

where δ is the wave number, Re is the Reynold number, M is the magnetic field, ∅ is the phase difference, and Dais the Darcy number.

Then, in view of Eq. (15), Eq. (1), (2), and (8) to (13) take the form:

The equation (1) becomes:

$$h_1(x,t) = 1 - a\,sin(2\pi x)\ . \quad (16)$$

The equation (2)becomes:

$$h_2(x,t) = -E_2 - b\,sin(2\pi x + \emptyset)\ . \quad (17)$$

The equation (8) becomes:

$$s_{xx} = 2\delta \frac{\partial u}{\partial x} + \frac{2\delta R_n(\frac{\partial u}{\partial x})}{\sqrt{2\delta^2\left(\frac{\partial u}{\partial x}\right)^2 + \left(\delta^2 \frac{\partial v}{\partial x} + \frac{\partial u}{\partial y}\right)^2 + 2\delta^2\left(\frac{\partial v}{\partial y}\right)^2}} . \quad (18)$$

The equation (*9*) becomes:

$$s_{xy} = \left(\delta^2 \frac{\partial v}{\partial x} + \frac{\partial u}{\partial y}\right) + \frac{R_n\left(\delta^2 \frac{\partial v}{\partial x} + \frac{\partial u}{\partial y}\right)}{\sqrt{2\delta^2\left(\frac{\partial u}{\partial x}\right)^2 + \left(\delta^2 \frac{\partial v}{\partial x} + \frac{\partial u}{\partial y}\right)^2 + 2\delta^2\left(\frac{\partial v}{\partial y}\right)^2}} . \quad (19)$$

The equation (*10*) becomes:

$$s_{yy} = 2\delta \frac{\partial v}{\partial y} + \frac{2\delta R_n(\frac{\partial v}{\partial y})}{\sqrt{2\delta^2\left(\frac{\partial u}{\partial x}\right)^2 + \left(\delta^2 \frac{\partial v}{\partial x} + \frac{\partial u}{\partial y}\right)^2 + 2\delta^2\left(\frac{\partial v}{\partial y}\right)^2}} . \quad (20)$$

The equation (11) becomes:

$$\frac{\partial u}{\partial x} + \frac{\partial v}{\partial y} = 0 . \quad (21)$$

The equation (12) becomes:

$$Re\,\delta\left(\frac{\partial u}{\partial t} + u\frac{\partial u}{\partial x} + v\frac{\partial u}{\partial y}\right) - \frac{\rho d^2}{\mu}\Omega^2 u - (2\Omega\delta^2 Re)\left(\frac{\partial v}{\partial t}\right) = -\frac{\partial p}{\partial x} + \delta^2 \frac{\partial}{\partial x} s_{xx} + \frac{\partial}{\partial y} s_{xy} - u\left(M^2 + \frac{1}{D_a}\right). \quad (22)$$

The equation (13) becomes:

$$Re\,\delta^3\left(\frac{\partial v}{\partial t} + u\frac{\partial v}{\partial x} + v\frac{\partial v}{\partial y}\right) - \frac{\rho d^2}{\mu}\delta^2\Omega^2 v - (2\Omega\delta^2 Re)\left(\frac{\partial u}{\partial t}\right) = -\frac{\partial p}{\partial y} + \delta^2 \frac{\partial}{\partial x} s_{xy} + \delta \frac{\partial}{\partial y} s_{yy} - v\delta^2\left(M^2 + \frac{1}{D_a}\right) \quad (23)$$

The relations establish a connection between the velocity components and stream function (ψ):

$$u = \partial\psi / \partial y \qquad v = -\partial\psi/\partial x. \quad (24)$$

Substituted Eqs. (24) in Eqs. (18), (19), (20), (21), (22), (23), respectively.

$$s_{xx} = (2\delta)\frac{\partial^2\psi}{\partial x\partial y} + \frac{2\delta R_n\left(\frac{\partial^2\psi}{\partial x\partial y}\right)}{\sqrt{2\delta^2\left(\frac{\partial^2\psi}{\partial x\partial y}\right)^2 + \left(-\delta^2 \frac{\partial^2\psi}{\partial x^2} + \frac{\partial^2\psi}{\partial y^2}\right)^2 + 2\delta^2\left(-\frac{\partial^2\psi}{\partial x\partial y}\right)^2}} . \quad (25)$$

$$s_{xy} = \left(-\delta^2 \frac{\partial^2\psi}{\partial x^2} + \frac{\partial^2\psi}{\partial y^2}\right) + \frac{R_n\left(-\delta^2 \frac{\partial^2\psi}{\partial x^2} + \frac{\partial^2\psi}{\partial y^2}\right)}{\sqrt{\delta^2\left(\frac{\partial^2\psi}{\partial x\partial y}\right)^2 + \left(-\delta^2 \frac{\partial^2\psi}{\partial x^2} + \frac{\partial^2\psi}{\partial y^2}\right)^2 + 2\delta^2\left(-\frac{\partial^2\psi}{\partial x\partial y}\right)^2}} . \quad (26)$$

$$s_{yy} = -\delta \frac{\partial^2\psi}{\partial x\partial y} + \frac{2\delta R_n\left(\frac{\partial^2\psi}{\partial x\partial y}\right)}{\sqrt{\delta^2\left(\frac{\partial^2\psi}{\partial x\partial y}\right)^2 + \left(-\delta^2 \frac{\partial^2\psi}{\partial x^2} + \frac{\partial^2\psi}{\partial y^2}\right)^2 + 2\delta^2\left(-\frac{\partial^2\psi}{\partial x\partial y}\right)^2}} . \quad (27)$$

$$\frac{\partial^2\psi}{\partial x\partial y} - \frac{\partial^2\psi}{\partial x\partial y} = 0 . \quad (28)$$

$$Re\,\delta\left(\frac{\partial^2\psi}{\partial t\partial y} + \frac{\partial^3\psi}{\partial x\partial y^2} - \frac{\partial^3\psi}{\partial x\partial y^2}\right) - \frac{\rho d^2}{\mu}\Omega^2 \frac{\partial\psi}{\partial y} - (2\Omega\delta^2 Re)\left(\frac{\partial^2\psi}{\partial t\partial x}\right) = -\frac{\partial p}{\partial x} + \delta^2 \frac{\partial}{\partial x} s_{xx} + \frac{\partial}{\partial y} s_{xy} - \frac{\partial\psi}{\partial y}\left(M^2 + \frac{1}{D_a}\right) . \quad (29)$$

$$Re\,\delta^3\left(-\frac{\partial^2\psi}{\partial t\partial x} + \frac{\partial^3\psi}{\partial x^2\partial y} - \frac{\partial^3\psi}{\partial x^2\partial y}\right) + \frac{\rho d^2}{\mu}\delta^2\Omega^2 \frac{\partial\psi}{\partial x} - (2\Omega\delta^2 Re)\left(\frac{\partial^2\psi}{\partial t\partial y}\right) = -\frac{\partial p}{\partial y} + \delta^2 \frac{\partial}{\partial x} s_{xy} + \delta \frac{\partial}{\partial y} s_{yy} - \frac{\partial\psi}{\partial x}\delta^2\left(M^2 + \frac{1}{D_a}\right) . \quad (30)$$

The dimensionless and boundary condition in the wave farms is [18]:

$$\psi = F/2\ ,\ \partial\psi / \partial y\ = -1\ at\ y = h_1 . \quad (31)$$

$$\psi = -F\ /\ 2\ ,\ \partial\psi / \partial y\ = -1\ at\ y = h_2 . \quad (32)$$

5. Solution of the Problem

It is impossible to provide a precise answer for each of the random parameters involved. We take perturbation strategy to get the answer. We go beyond treating the disorder.

$$\psi = \psi_0 + R_n\,\psi_1 + O({R_n}^2),$$
$$F = F_0 + R_n F_1 + O({R_n}^2)\ . \quad (33)$$

Substitute the terms (33) into Eqs. (25)-(30), and the equations for the boundary conditions (31) and (32) ($\delta \ll 1$), Due to the fact that higher order components involve the power of (δ) is lower and negligible, we may construct by equating the coefficients of the following system of equivalent powers Re:

From Eq. (26) and Eq. (29) we get:

$$\frac{dp}{dx} = \eta\psi_y + \psi_{yyy} + R_n\,\psi_y - \beta\,\psi_y\ . \quad (34)$$

$$\eta = \frac{(\Omega^2 d^2 \rho)}{\mu}\ . \quad (35)$$

$$\beta = M^2 + \frac{1}{Da}\ . \quad (36)$$

From differential of y for Eq. (34), we get

$$0 = \psi_{yyyy} + R_n\,\psi_{yy} - \beta\,\psi_{yy} + \eta\psi_{yy}\ . \quad (37)$$

From Eq (30) we get:

$$-\frac{\partial p}{\partial y} = 0\ . \quad (38)$$

6. Zero Order System

When the order's terms are R_n that are trivial in the system of zeroth order, we obtain:

$$\psi_{0yyyy} - \beta\,\psi_{0yy} + \eta\,\psi_{0yy} = 0\ . \quad (39)$$

Such that

$\psi_0 = F_0 / 2$, $\partial\psi_0 / \partial y = -1$ at y= h_1 and
$\psi_0 = -F_0 / 2$, $\partial\psi_0 / \partial y = -1$ at y= h_2 . (40)

7. First order system

$$\psi_{1_{yyyy}} + \psi_{0yy} - \beta\,\psi_{1yy} + \eta\,\psi_{1_{yy}} = 0. \quad (41)$$

$$\psi_{1_{yyyy}} - \beta\,\psi_{1yy} + \eta\,\psi_{1_{yy}} = -\psi_{0yy}\ . \quad (42)$$

$\psi_1 = F_1 / 2$, $\partial\psi_0 / \partial y = -1$ at y= h_1 and
$\psi_1 = -F_1 / 2$, $\partial\psi_0 / \partial y = -1$ at y= h_2 . (43)

And by resolving the related zeroth and first order systems, you may obtain the final equation for the stream function:

$$\psi = \psi_0 + R_n\,\psi_1. \quad (44)$$

Where the functions (ψ_0, ψ_1) hefty expressions Consequently, they will be mentioned in Appendix. Eqs. (29) can be written as

$$\frac{\partial p}{\partial x} = \psi_{0yyy} + R_n\psi_{1yyy} + R_n\psi_{0yy} + {R_n}^2\psi_{0yy} - \beta\,\psi_{0y} + \eta\psi_{0y} - \beta R_n\psi_{1y} + \eta R_n\psi_{1y}\ . \quad (45)$$

The definition of pressure increases per wave length (Δp) is

$$\Delta p = \int_0^1 \frac{dp}{dx}\,dx. \quad (46)$$

8. Results and discussions

To investigate the impact of physical factors like the effect of the Darcy number (Da), Reynolds number (Re), Rotation (Ω), Porous medium parameter (k), Material fluid parameters (Rn), Density (ρ), Viscosity (μ) Magnetic field (M) and phase difference ($\emptyset$), the plotted axial velocity (u), pressure rise (Δp) and stream function (ψ) in Figures 2-18 are illustrated using the software MATHEMATICA.

8.1 Velocity Distribution (u)

Figures 2, 3, and 9 show the effect of variation in viscosity (Ω), (Da) and (d) on the velocity axial (u), at the lower part of the channel the viscosity increase but the velocity decrease and in the rest part of velocity increase by viscosity increase. Figure 4 shows that the axial velocity increases with an increase in (Rn). Figure 5 shows that the axial speed with increasing (M) increases in the central area of the canal, while the axial velocity decreases at the boundaries of the canal wall. Figure 6 shows the effect of (ρ) when axial speed increases, it starts decreasing and then it is combined with the other. Figure 7 the effect of (∅) when the speed increases, it starts decreasing at the left channel wall, then it merges with the other one in the center, and then increases at the right channel wall. Figure 8 shows that axial speed with increasing (E) decreases in the central area of the canal, while axial velocity increases at the boundaries of the canal wall.

8.2 Pressure Rise (Δ**p**)

Figures 10–13 display the various pressure increases in the wave outline's capability of volumetric stream rate for various Darcy number (Da), Rotation (Ω), material fluid parameter (Rn), magnetic field (M) and phase difference (∅). The link between the non-dimensional average pressure rises per wavelength and the dimensionless mean flow rate (Q1) with variation in the interesting parameters included in (Δp) will be demonstrated in this subsection. Figure10 shows the effect of increasing the parameter (Rn) on (ΔP) revealing that pressure rice per wave length ΔP increases in magnitude in all regions. Figure 11 demonstrates that pressure increase (Δp) diminishes as (Da) In the zone of increased pumping and the compounding region ($\Delta p < 0$), it is seen that pumping rises. According to Figure 12, the pumping rate decreases in a cop umping zone where ($\Delta p < 0, Q1 < 0$) with an increase in (M) and increases in a retrograde region where ($\Delta p > 0, Q1 > 0$), as seen in the graph. The pressure rises ($\Delta p > 0$) increases as the magnetic field (M) grows. Figure 13 shows the pressure rice per wave length ΔP decreases in magnitude for fixed values of the viscosity ∅.

8.3 Trapping phenomenon

An interesting component happens in peristaltic flows closed movement strains lure bolus, or the extent of fluid called a bolus, in the channel tube close to the partitions, and this trapping bolus advances along the path of the wave. In Figures 14 –18, plots of the streamlines are shown at different values of (Ω), (Da), (Rn), (M), and (∅). Figure 14 shows that trapping exists in the channel's midpoint and that decreases the size of the trapping bolus as (Da) increases. Figures 16-18 show the exhibits that the trapping exists in the focus of the channel, we perceive that the size of the growing trapping bolus with increasing (Ω), (∅), (Rn) and open channel with ($\Omega = 1.1$), ($\emptyset = \pi/2$), ($Rn = 0.5$). Figure 15 shows that trapping exists in the channel's midpoint and that the size of the trapping bolus shrinks and expands as (M) increase

9. Conclusions

The peristaltic motion of the Bingham plastic fluid in an asymmetric channel with a porous material was examined. In this study, we determine the impact of magnetism and rotation on it. By choosing peristaltic waves with various ranges, phases, low Reynolds numbers, and wavelengths, the asymmetric duct is created. The expression for the axial velocity, magnetic force, flow function, and current density was also obtained using an application of the perturbation method. Graphs are used to illustrate the findings as follows:

A. The velocity profile increases in view of an increase in Ω, *R*n, Da, and ∅. However, it decreases with increasing *M*.

B. When increasing the speed relative to density (ρ) it starts decreasing and then remains constant.
C. The pressure rice per wave length ΔP decreases in magnitude for fixed values of the viscosity $\emptyset$ shows the effect of increasing the parameter Rn on ΔP reveals that pressure rice per wave length ΔP increases in magnitude in all regions.
D. According to the parameters that are being employed, it is seen that the volume of the trapped bolus starts to decay and rise.
E. There are several applications for peristaltic movement in both engineering and physical sciences. These waves, which spread throughout the length of an extensible tube and mix and transport fluid in the wave's direction, are really produced by the expansion and contraction of the extensible tube. The ureter and extracorporeal blood circulation are two tubular organs in the human body where this process takes place.

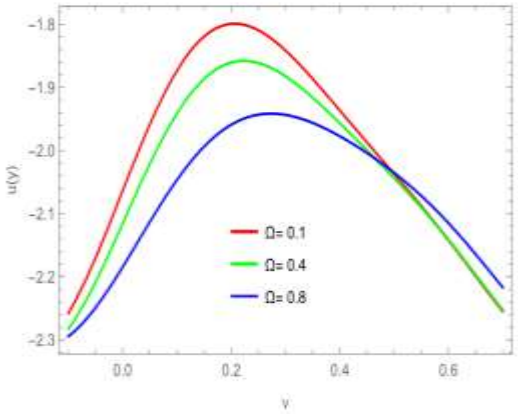

Fig. 2. Variation of velocity for different values of Ω when Da = 6, Rn= 0.5, M = 1, ρ =1, $\emptyset$ = 1.5, a = 0.1, b = 0.3, d =0.5, E=0.1, μ = 1.

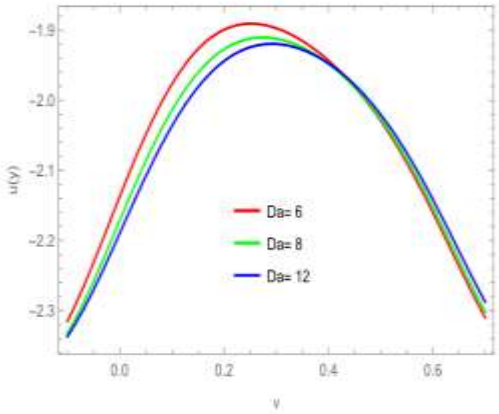

Fig. 3. Variation of velocity for different values of Da when Ω= 0.5, Rn= 0.5, M = 1, ρ =1, $\emptyset$ = 1.5, a = 0.1, b = 0.3, d =0.5, E=0.1, μ = 1.

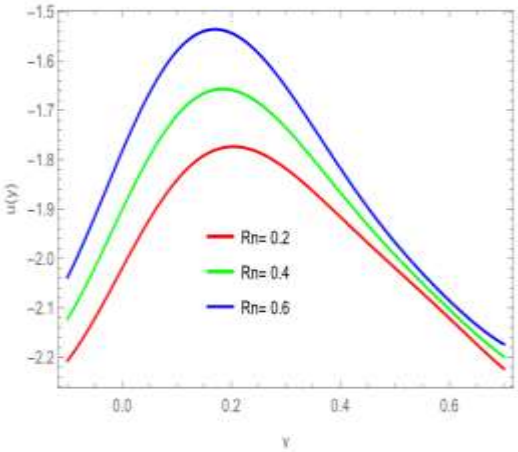

Fig. 4. Variation of velocity for different values of Rn when Da = 6, M= 1, Ω= 0.5, ρ =1, $\emptyset$ = 1.5, a = 0.1, b = 0.3, d =0.5, E=0.1, μ = 1.

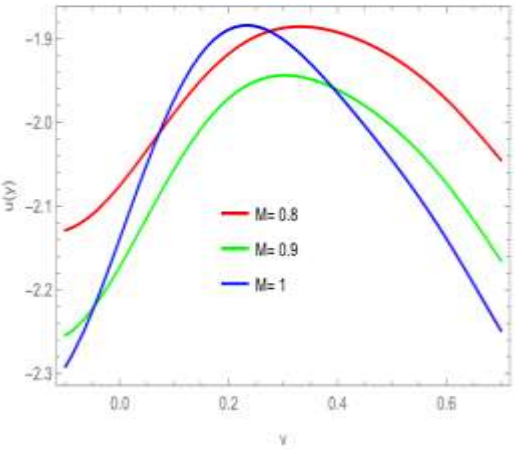

Fig. 5. Variation of velocity for different values of *M* when Da = 6, Rn= 0.5, Ω= 0.5, ρ =1, $\emptyset$ = 1.5, a = 0.1, b = 0.3, d =0.5, E=0.1, μ = 1.

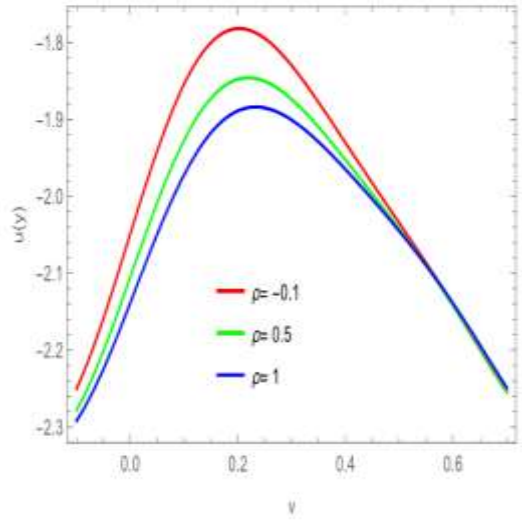

Fig. 6. Variation of velocity for different values of v when Da = 6, Rn= 0.5, M = 1, Ω= 0.5, Ø = 1.5, a = 0.1, b = 0.3, d =0.5, E=0.1, μ = 1.

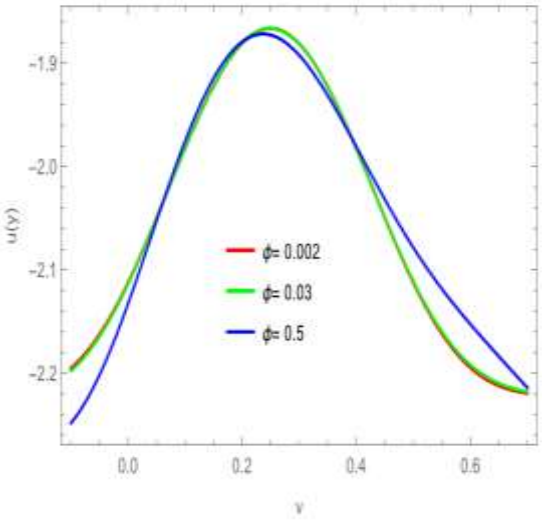

Fig. 7. Variation of velocity for different values of Ø when Da = 6, M= 1, Ω= 0.5, ρ =1, Rn= 0.5, a = 0.1, b = 0.3, d =0.5, E=0.1, μ = 1.

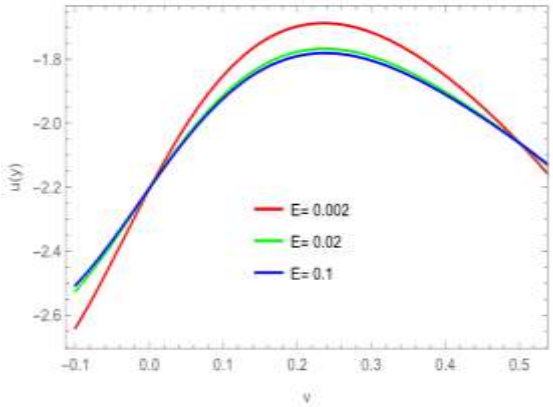

Fig. 8. Variation of velocity for different values of E when Da = 6, Rn= 0.5, M = 1, Ω= 0.5, Ø = 1.5, a = 0.1, b = 0.3, d =0.5, ρ =1, μ = 1.

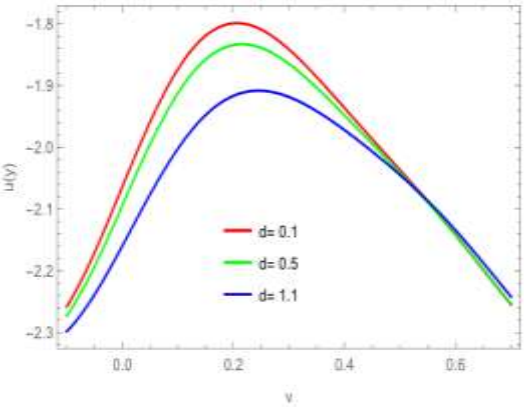

Fig. 9. Variation of velocity for different values of d when Da = 6, Rn= 0.5, M = 1, Ω= 0.5, Ø = 1.5, a = 0.1, b = 0.3, ρ=1, E=0.1, μ = 1.

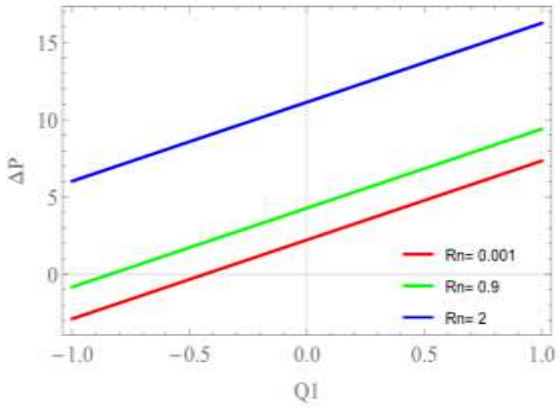

Fig. 10. Variation of pressure rise ΔP with Q1 for different values of Rn when Ω= 0.5, Da= 0.9, M = 2, ρ=0.4, Q=1.5, Ø = 0.4, a = 0.3, b = 0.3, d =0.5, E=0.1, μ = 1.

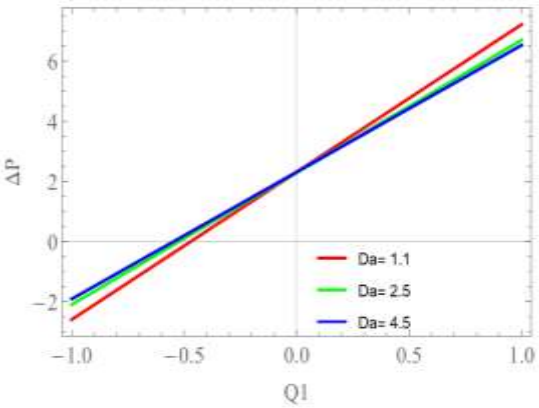

Fig. 11. Variation of pressure rise ΔP with Q1 for different values of Da when Ω= 0.5, Rn= 0.1, M = 2, ρ=0.4, Q=1.5, Ø = 0.4, a = 0.3, b = 0.3, d =0.5, E=0.1, μ = 1.

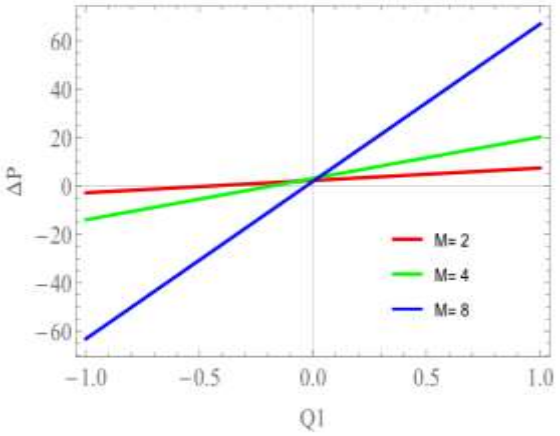

Fig. 12. Variation of pressure rise ΔP with Q1 for different values of M when Ω= 0.5, Rn= 0.1, Da= 0.9, ρ =0.4, Q=1.5, Ø = 0.4, a = 0.3, b = 0.3, d =0.5, E=0.1, μ = 1.

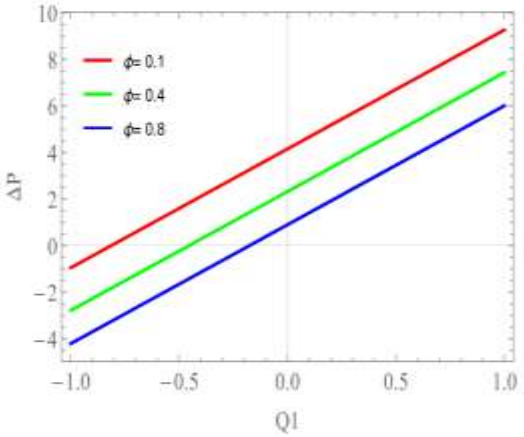

Fig. 13. Variation of pressure rise ΔP with Q1 for different values of Ø when Ω= 0.5, Da= 0.9, M = 2, ρ =0.4, Q=1.5, Rn = 0.1, a = 0.3, b = 0.3, d =0.5, E=0.1, μ = 1.

(a) **(b)**

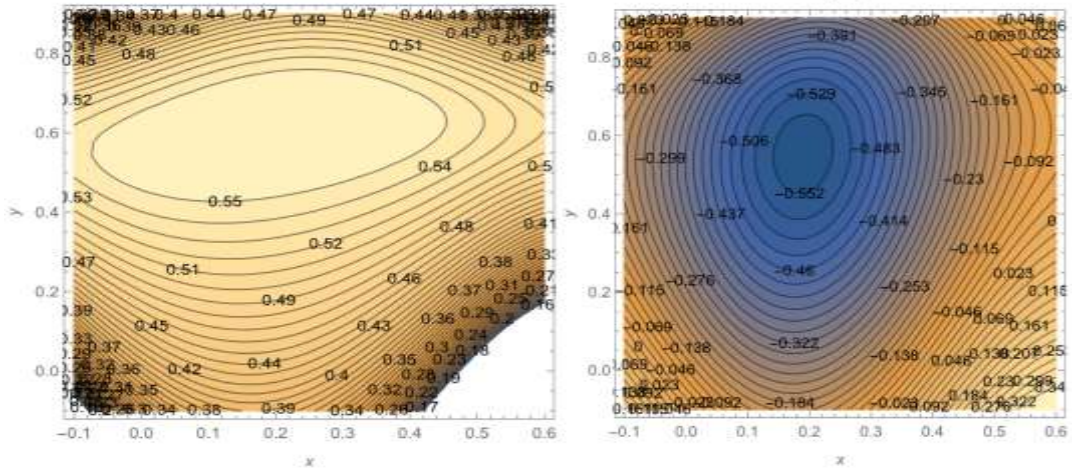

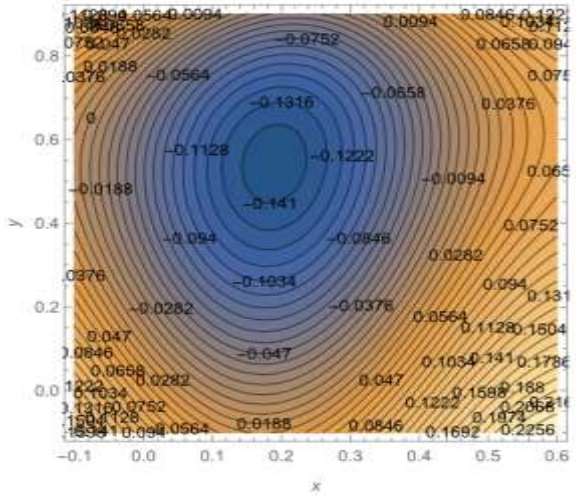

(c)

Figure 14. stream function in the wave frame of (Da) such that in (a) Da =0.2, (b) Da=3.5, (c) Da =4.5, in Ω= 0.5, Rn= 0.1, M = 0.1, v =0.4, Ø = 0.5, a = 0.1, ρ = 0.3, d =0.5, E=0.1, μ

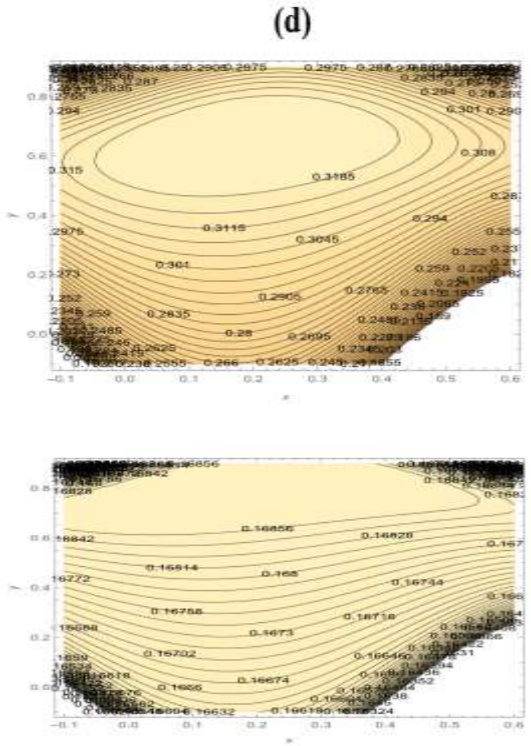

Figure 15. stream function in the wave frame of (M) such that in (d) M =2, (e) M=4, (f) M =8, in Ω= 0.5, Rn= 0.1, Da = 0.2, ρ =0.4, Ø = 0.5, a = 0.1, b = 0.3, d =0.5, E=0.1, μ = 1.

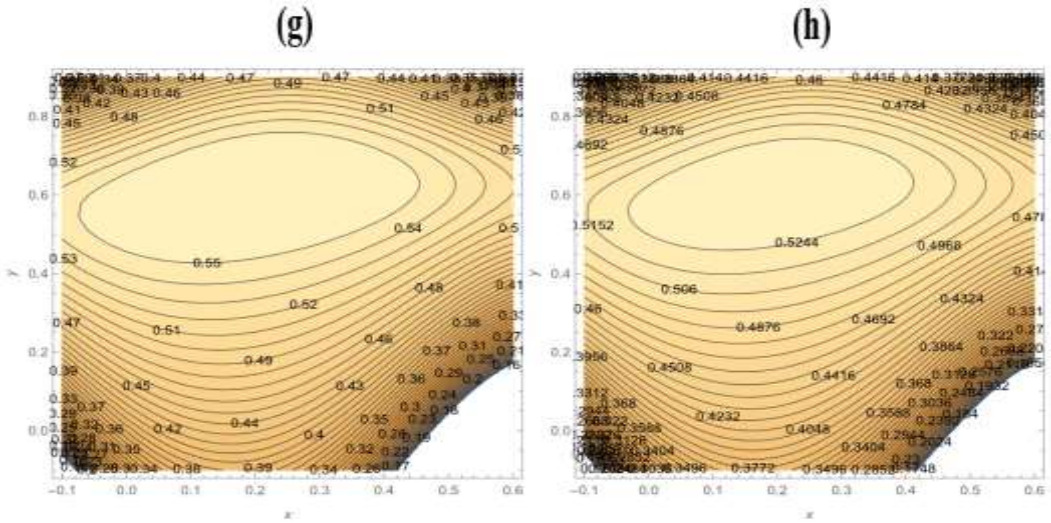

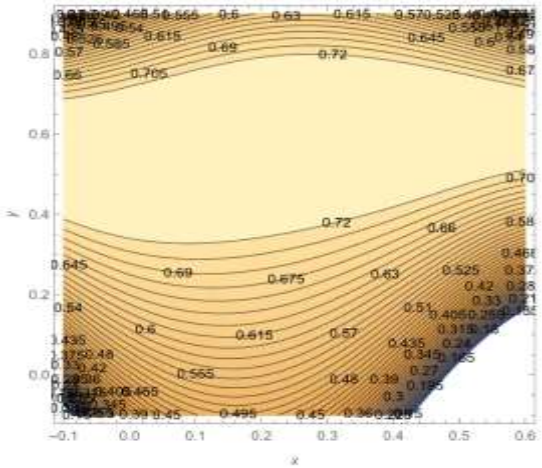

Figure 16. stream function in the wave frame of (Ω) such that in (g) Ω =0.1, (h) Ω =0.5, (i) Ω =1.1, in such that in M= 0.1, Rn= 0.1, Da = 0.2, ρ=0.4, Ø = 0.5, a = 0.1, b = 0.3, d =0.5, E=0.1, μ = 1.

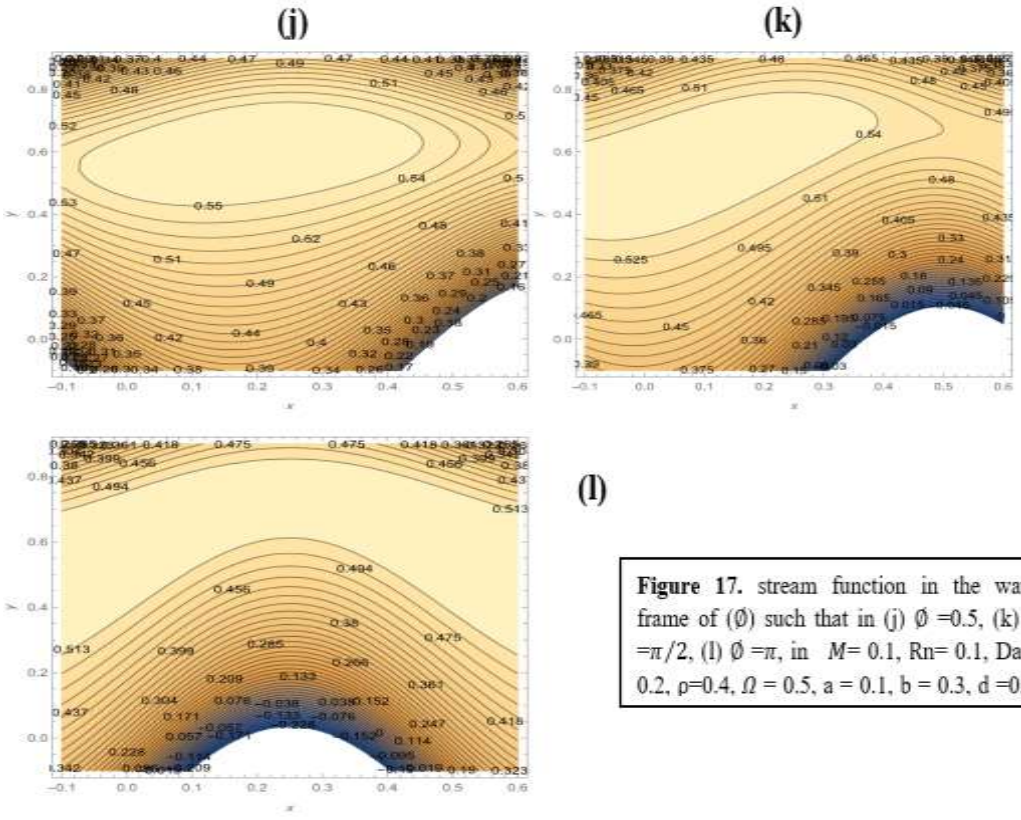

Figure 17. stream function in the wave frame of (Ø) such that in (j) Ø =0.5, (k) Ø =$\pi/2$, (l) Ø =π, in M= 0.1, Rn= 0.1, Da = 0.2, ρ=0.4, Ω = 0.5, a = 0.1, b = 0.3, d =0.5,

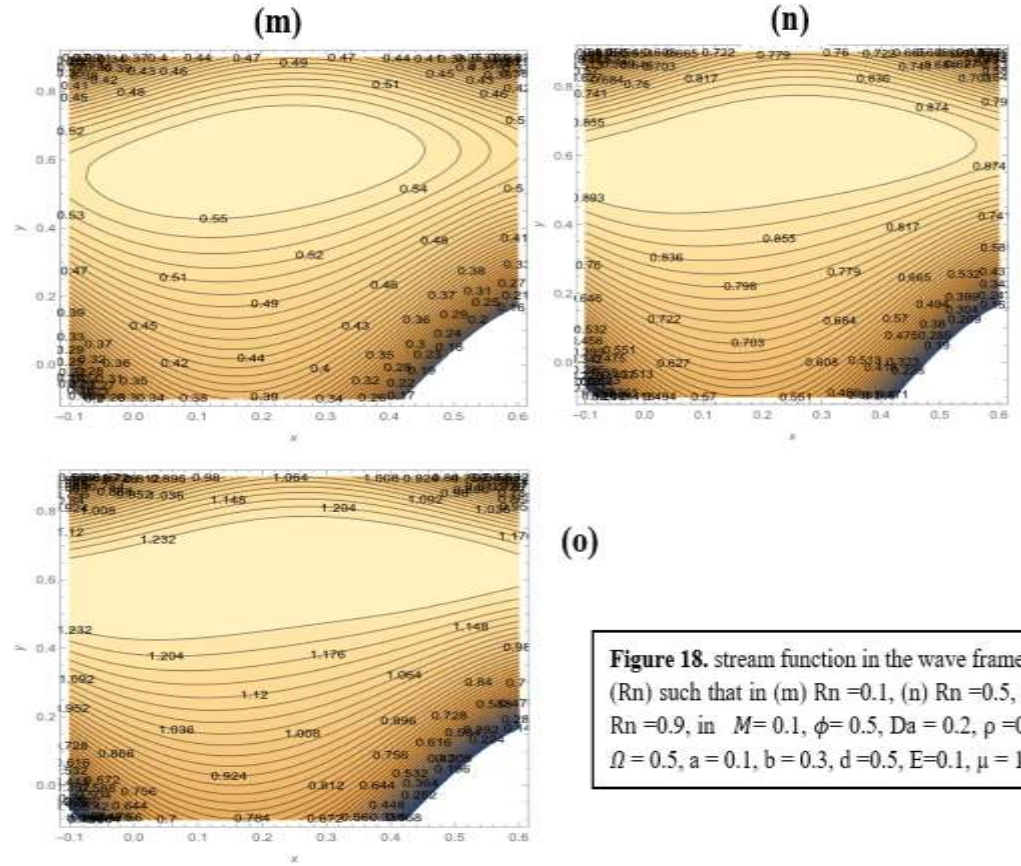

Figure 18. stream function in the wave frame of (Rn) such that in (m) Rn =0.1, (n) Rn =0.5, (o) Rn =0.9, in M= 0.1, ϕ= 0.5, Da = 0.2, ρ =0.4, Ω = 0.5, a = 0.1, b = 0.3, d =0.5, E=0.1, μ = 1.

References

[1] T. W. Latham, *Fluid motions in a peristaltic pump. Diss. Massachusetts Institute of Technology,* 1966.

[2] T. Parkes and J. C. Burns, "Peristaltic motion," *Journal of Fluid Mechanics,* vol. 29, no. 4, pp. 731-743, 1967.

[3] A. H. Shapiro, "Peristaltic pumping with long wavelength at low Reynolds number," *Fluid Mech.,* vol. 37, pp. 799-825, 1969.

[4] M. Faraday, "Experimental Researches in Electricity," *Phil. Trans.,* vol. 15, p. 175, 1832.

[5] A. M. Abd-Alla, S. M. Abo-Dahab and H. D. El-Shahrany, "Effects of rotation and initial stress on peristaltic transport of fourth grade fluid with heat transfer and induced magnetic field," *Journal of Magnetism and magnetic Materials,* vol. 349, pp. 268-280, 2014.

[6] A. M. Abdulhadi and H. A.-H. Aya , "Effects of rotation and MHD on the Nonlinear Peristaltic Flow of a Jeffery Fluid in an Asymmetric Channel through a Porous Medium," no. 57.1A, pp. 223-240, 2016.

[7] M. . A.-A. A and M. A.-D. S, "Rotation effect on peristaltic transport of a Jeffrey fluid in an asymmetric channel with gravity field," *Alexandria Engineering Journal,* no. 55.2, pp. 1725-1735, 2016.

[8] A. H, A. A, H. Zahir and T. Hayat, "Hall current and Joule heating effects on peristaltic flow of viscous fluid in a rotating channel with convective boundary conditions," *Results in physics,* no. 7, pp. 2831-2836, 2017.

[9] S. A. T, "Impress of rotation and an inclined MHD on waveform motion of the non-Newtonian fluid through porous canal," *Journal of Physics,* vol. 1591, no. 1, 2020.

[10] A. M. Abdulhadi and S. . A. Tamara , "Effect of magnetic field on peristaltic flow of Walters' B fluid through a porous medium in a tapered asymmetric channel," *Journal of advances in Mathematics,* no. 1.12, pp. 6889-6893, 2017.

[11] M. A. Murad and A. M. Ahmed , "Influence of heat and mass transfer on peristaltic transport of viscoplastic fluid in presence of magnetic field through symmetric channel with porous medium," *Journal of Physics,* vol. 1804, no. 1, 2021.

[12] L. Z. Hummady and R. R. afa , "Influence of inclined magnetic filed on peristaltic flow of a hyperbolic tangent fluidin ati-symmetric channel with porus medium," *International Journal of Advanced Science and Technology,* vol. 29, no. 02, pp. 2525-2536 , 2020.

[13] M. A. Ahmed and H. N. Mohaisen, "Effects of the Rotation on the Mixed Convection Heat Transfer Analysis for the Peristaltic Transport of Viscoelastic Fluid in Asymmetric Channel," *Iraqi Journal of Science,* vol. 63, no. 3, pp. 1240-1257, 2022.

[14] H. N. Mohaisen and M. A. Ahmed , "Influence of the Induced Magnetic and Rotation on Mixed Convection Heat Transfer for the Peristaltic Transport of Bingham plastic Fluid in an Asymmetric Channel," *Iraqi Journal of Science,* vol. 63, no. 4, pp. 1770-1785, 2022.

[15] K. Vajravelu, S. Sreenadh, P. Devaki and K. V. Prasad, "Peristaltic pumping of a Casson fluid in an elastic tube," *Journal of Applied Fluid Mechanics,* vol. 9, no. 4, pp. 1897-1905, 2016.

[16] B. Sumalatha and S. Sreenadh, "Poiseuille flow of a Jeffery fluid in an inclined elastic tube," *International Journal of Engineering Sciences and Research Technology,* no. 07, pp. 150-160, 2018.

[17] Y. Wang, "Time-dependent Poiseuille flows of visco-elasto-plastic fluids," vol. Acta mechanica 186.1, pp. 187-201, 2006.

[18] F. M. White, "Fluid Mechanics," *McGraw-Hill,* no. New York, 1994.